University of California

Santa Cruz

Characterization of the H_2 production activity in *Rhodopseudomonas palustris*

A thesis submitted in partial satisfaction

of the requirements for the degree of

Masters of Arts

in

Molecular Cell and Developmental Biology

By

Phillip Wang

June 2017

The thesis of Phillip Wang

is approved:

_____

Professor Barry Bowman, Chair

_____

Professor Chad Saltikov

_____

Professor Alan Zahler

_____

Tyrus Miller

Vice Provost and Dean of Graduate Students

Table of Contents

Abstract v

Acknowledgement vi

Introduction 1

Hydrogenic Enzymes 2

Nitrogenase 2

Hydrogenase 5

Hyq Hydrogenase 6

Photo-Hydrogenic Bacteria 9

Rhodopseudomonas palustris 10

Results 14

Conclusion 33

References 34

List of Figures

Figure 1: The Nitrogen Cycle 3

Figure 2: Mo-dinitrogenase Crystal Structure 4

Figure 3: Hydrogenase Metal Co-factors 5

Figure 4(A-C): Comparison of bacterial Complex I with Hyq 9

Figure 5: Main metabolic modes of *R. palustris* 10

Figure 6: Proposed electron pathway for Hyq relative to PS II 13

Figure 7: Chemoheterotrophic vs. Photoheterotrophic cultures 16

Figure 8: RT-PCR of *hyq* and *nif* 17

Figure 9: H_2 measurement of HaA2 and mutant derivatives 18

Figure 10: OD660 of HaA2 in defined media 20

Figure 11A: OD660 of HaA2 in modified media +/- 3mM thiosulfate 21

Figure 11B: OD660 of HaA2 in photoautotrophic conditions 22

Figure 12: H_2 measurement for HaA2+/- 3mM sodium thiosulfate..... 24

Figure 13: H_2 measurement for washed HaA2 +/- succinate..... 25

Figure 14: Diagram of the engineered nahR$^+$PnahG::hyq$^+$ construct..... 26

Figure 15: H_2 measurement for HaA2-117 with salicylate inducer 31

Figure 16: RT-PCR of hyq under various salicylate concentrations..... 32

Table 1: Relevant genotypes of HaA2 and mutant derivatives..... 19

Table 2: Synthetic oligodeoxynucleotide PCR primers..... 29

Abstract

Phillip Wang: Characterization of the H_2 production activity in *Rhodopseudomonas palustris*

Photosynthetic purple bacteria, such as Rhodobacter, Rhodopseudomonas, and Rhodospirillum are among the various types of hydrogen producing microbes that are anoxygenic phototrophs and capable of using light for H_2 production. Here we report that Rhodopseudomonas palustris strain HaA2 encodes for a novel hydrogenase (*hyq*) that can produce H_2 under phototrophic conditions. In addition to the hyq operon, R. palustris HaA2 also possesses the known molybdenum dinitrogenase complex (*nif*), which produces H_2 as an obligate byproduct of N_2 fixation. Through a series of deletion mutants only the Nif and Hyq enzymes produced H_2 in HaA2, under all the conditions tested. Furthermore, H_2 production in HaA2 can be driven by succinate oxidation, but not thiosulfate under the conditions tested.

Acknowledgements

I would like to dedicate this thesis to Professor Robert A. Ludwig (Bob), who was an inspiration and role model to the many people that he met and taught. Bob was a man with iron-like principles, admirable morals, kind heart, and a world class mind. What a blessing that you and I were alive at the same time.

Introduction

With the well documented research on climate change, the vast majority of the literature has pinpointed carbon dioxide (CO_2) generated by human activities as the primary factor driving global warming **[1]**. Because the majority of the human derived CO_2 emission stems from the combustion of fossil fuel, the transition to renewable alternatives must keep pace with our growing energy demand. Dihydrogen gas (H_2) is a high energy molecule that holds many positive attributes as an alternative energy carrier. In comparison to octane, the theoretical energy yield from the combustion of H_2 with a mole of oxygen (O_2) offers a slight energetic advantage, 486 kJ vs. 409 kJ per mole O_2. Furthermore, this energy difference is greater in practice because the combustion of H_2 results in H_2O as the sole product, whereas the combustion of octane yields a mixture of CO_2, carbon monoxide, and other greenhouse gases that lower the actual energy yield obtained from octane. Among the of zero-carbon renewable energy sources, solar energy has the most potential over other forms of renewable energy by at least 2 orders of magnitude **[2]**. Therefore, solar driven H_2 production provides a promising solution to capture and convert the vast but variable amounts of light energy into a chemical form that can be stored and distributed in response to supply and demand **[2]**.

Hydrogenic Enzymes

One approach for converting solar energy into H_2 is through the use of biological catalyst. In comparison to non-biological catalysts, hydrogenic enzymes are more robust and catalyze the endergonic formation of H_2 with much lower energy input **[3]**. To date, hydrogen producing enzymes belong in either the nitrogenase or hydrogenase enzyme family **[4,5]**. While dinitrogenases produce H_2 as a by-product of fixing dinitrogen (N_2), hydrogenases can oxidize or produce H_2 as the sole reaction. Research on the structure and characteristic of hydrogenic enzymes seek to address essential knowledge gaps and move society closer towards clean production of H_2 on a large scale **[3]**.

Nitrogenase

Of the three known types of dinitrogenase complexes, the molybdenum-dinitrogenase (Mo-dinitrogenase) is the best characterized enzyme complex **[6]**. Mo-dinitrogenase, encoded by the *nif operon,* catalyzes the reduction of atmospheric N_2 into biologically usable ammonium (NH_4^+) along with H_2 as an obligatory side product.

$$\mathbf{N_2 + 8e^- + 10H^+ + 16\ MgATP^{2-} \rightarrow 2NH_4^+ + H_2 + 16\ MgADP^- + 16\ Pi^-}$$

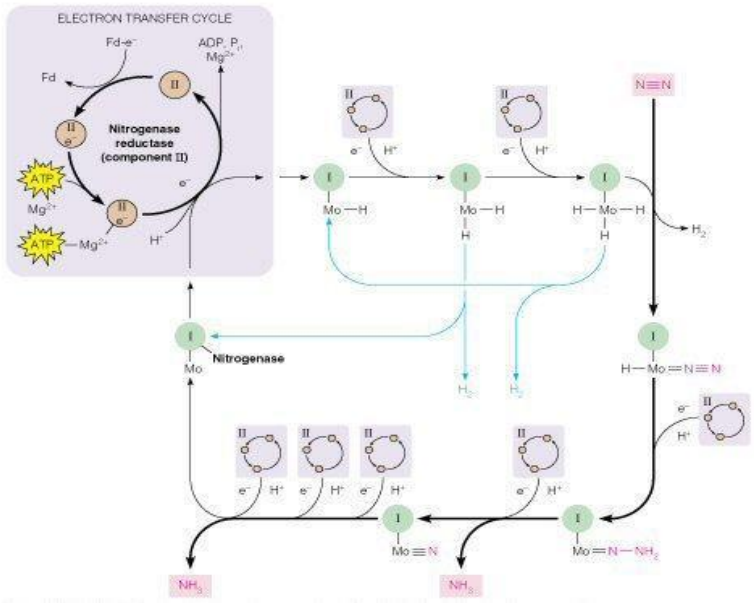

Fig 1: Multistep process of N_2 reduction by the Mo-dinitrogenase complex **[7].**

The Mo-dinitrogenase is composed of two enzymes, a dinitrogenase reductase and a dinitrogenase. The dinitrogenase reductase exists as a dimer of two identical subunits, each harboring a single [4Fe-4S] redox center and an ATP/ADP binding site. Since the triple bonded N_2 is relatively inert, the dinitrogenase reductase drives the reaction forward by hydrolyzing 2 ATP per electron transferred to the dinitrogenase. The dinitrogenase consists of an $\alpha_2\boldsymbol{\beta}_2$ tetramer, containing two Fe-Mo cofactors directly involved in the reduction of N_2. In the eight recursive single electron transfers to the dinitrogenase catalytic center, the first two electrons are used to reduce two H^+ to form one H_2. When H_2 is displaced by N_2, the subsequent six electrons, along with H^+, are used to reduce N_2 into two NH_4^+ **[7]**. In summary, one H_2 is

produced for every N_2 reduced, but this ratio varies with environmental conditions and also varies in the two other dinitrogenase complexes. While the primary reaction of the dinitrogenase complex is to reduce N_2 into usable NH_4^+, the obligatory H_2 produced in this process has motivated researchers to engineer the dinitrogenase complexes into more efficient producer of renewable energy **[8-10]**.

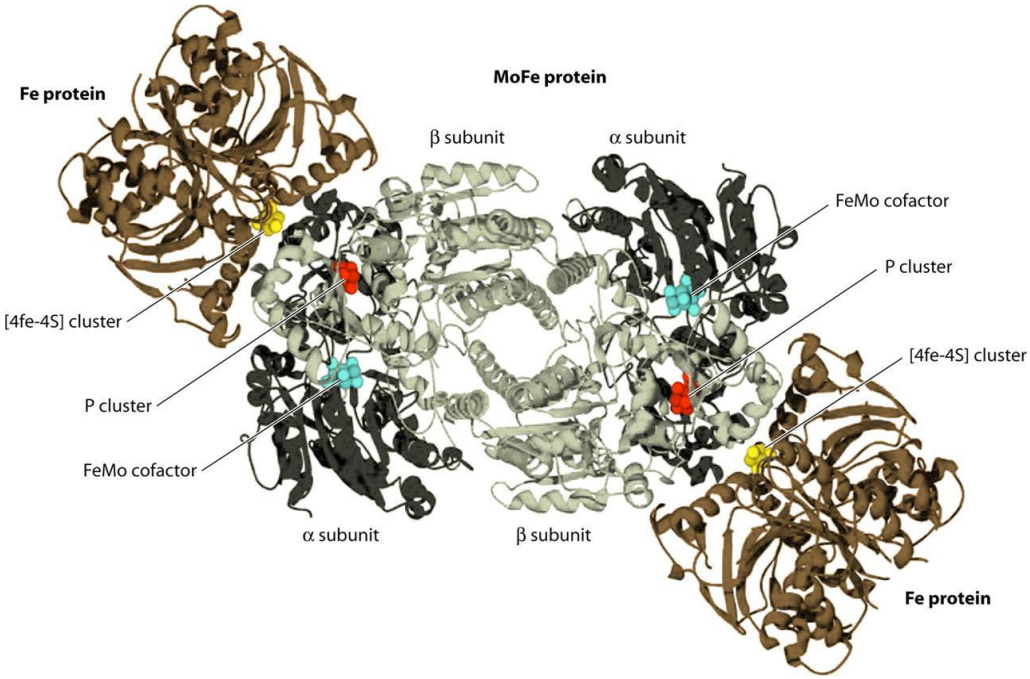

Fig 2: Crystal structure of the Mo-dinitrogenase complex of Azobacter vinelandii **[11]**.

Hydrogenase

Hydrogenases are metallo-enzymes involved in the direct oxidation and production of molecular H_2. The active site consists of an organic metallic center harboring a Ni-Fe, Fe-Fe, or Fe cofactor. These metal cofactors are coordinated by a combination of Cys residues and non-protein ligands (e.g. CO CN ligands). Accordingly, the various types of hydrogenases are classified by their respective active site metal cofactors **[5,12]**.

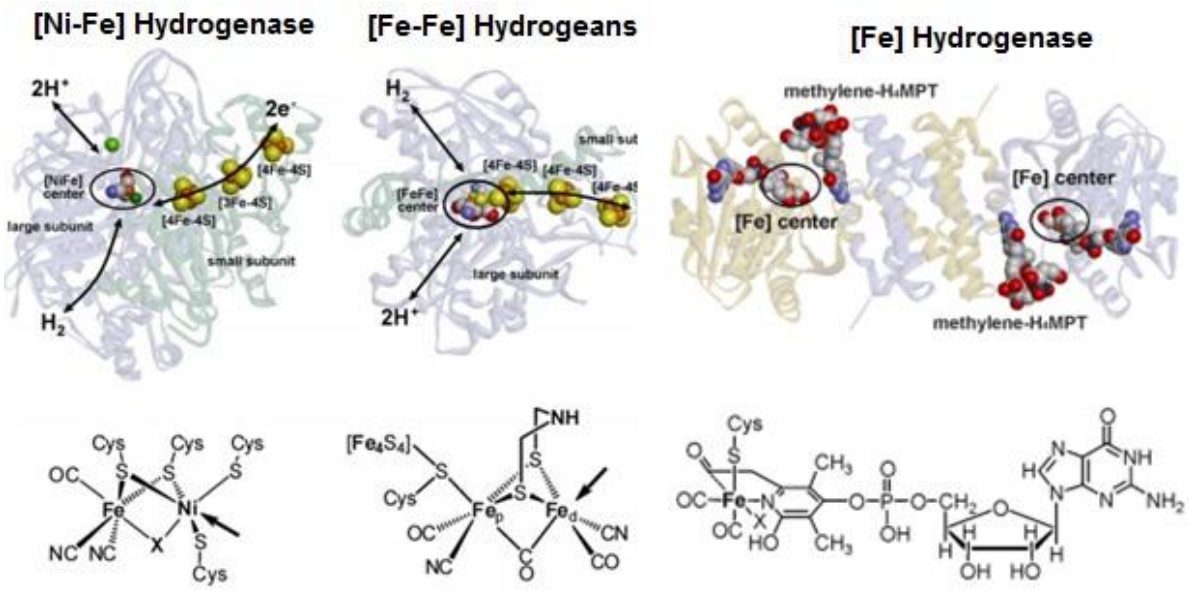

$$2H^+ + 2e^- \leftrightarrow H_2$$

Fig 3: Metal cofactors and the coordination by amino acid and non protein ligands in the three classes of hydrogenases **[13].**

Of relevance to this study are group I and IV [Ni-Fe] hydrogenases. Group I [Ni-Fe] hydrogenases can only oxidize H_2 and are characterized as

membrane-bound hydrogenases with their catalytic centers facing the periplasm [**12**]. Group IV [Ni-Fe] hydrogenases are membrane-integral hydrogenase with bidirectional H_2 oxidation and production activity. In addition, identified group IV [Ni-Fe] hydrogenases have homologous subunits to the core subunits of bacteria respiratory complex I [**12**].

Hyq Hydrogenase

Previously, we reported a novel membrane-integral hydrogenase (*hyq*) in the non-phototrophic *Azorhizobium caulinodans* and a few related diazotrophic micro-aerophilic α-*Proteobacteria* **[14−16]**. In *A. caulinodans* N_2 fixing cultures, *hyq* helps recycle endogenous H_2 produced by the soluble dinitrogenase complex, which converts N_2, H^+ ions, and metabolic low potential electrons, into H_2 and two NH_4^+ **[*7*]**. In turn, oxidation of the endogenously produced H_2 recycles energy through cellular respiration with O_2 as the terminal e^- acceptor **[14,15].** In contrast to group I uptake hydrogenases of diverse H_2 oxidizing bacteria **[14]**, the *in vivo* activity of *hyq* is reversible and has been demonstrated to produce H_2 in microaerobic *A. caulinodans* cultures when the respiratory membrane e^- carriers are highly reduced [**16**].

The Hyq hydrogenase of *Azorhizobium caulinodans* consists of six subunits encoded by *hyq*BCEFGI **[14]**. The six inferred structural proteins, HyqBCEFGI, are all homologous, averaging ~20% identity, with the core subunits of *Thermus thermophilus* respiratory complex I, NADH:quionone

oxidoreductase (Nqo, Fig 4A). The *Thermus thermophilus* Nqo is composed of fifteen subunits split into two subcomplexes, a membrane-integral L_o and a membrane-peripheral L_1. From the X-ray crystal structure of *Thermus thermophilus* Nqo [**17,18**], eight different proteins, Nqo1-6 and 9, form the membrane-peripheral L_1 subcomplex and faces the cytoplasm in order to oxidize NADH as the e^- donor. These eight subunits orient a string of Fe-S centers that couple the e^- transfer from NADH to membrane quinone. The membrane-integral L_o subcomplex is formed by seven different proteins, Nqo7-8 and 10-14, and helps mediate transmembrane H^+ pumping. Binding of quinone to Nqo is believed to occur in a cavity formed between a four-helix bundle of Nqo4, the H1 helix of Nqo6, and a transmembrane helix 1 of Nqo8 [**17**].

In comparison to the Hyq homologue, HyqG, HyqI, and HyqC appear to be homologous to Nqo4, Nqo6, and Nqo8, with 30%, 36%, and 31% identity, and 46%, 55%, and 49% similarity, respectively. Specifically, the most oxidized 4Fe4S center, N2, of Nqo6, believed to be the direct reducing agent for quinone, appears to be conserved in the HyqI protein sequence, based on the conservation of all four key cysteine residues in the sequences that house the cluster (Fig. 4C). Also, the three subunits of the L_o subcomplex involved in H^+ pumping are homologous to HyqE, HyqB, and HyqF, with key charged residues being conserved. Furthermore, the inferred HyqGI catalytic center would face the cell cytoplasm, similar to Nqo. Taken together, we

hypothesize that *hyq* represents a simplified core, membrane-integral H_2:quinone oxidoreductase with H^+ pumping activity [Fig 4B, **16**].

A)

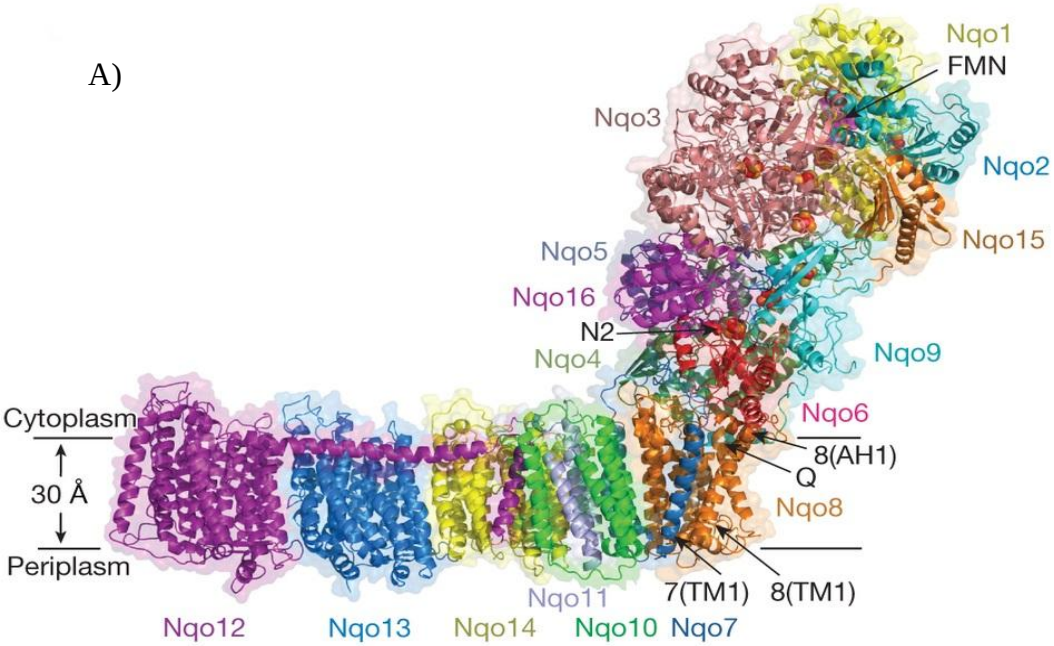

B)

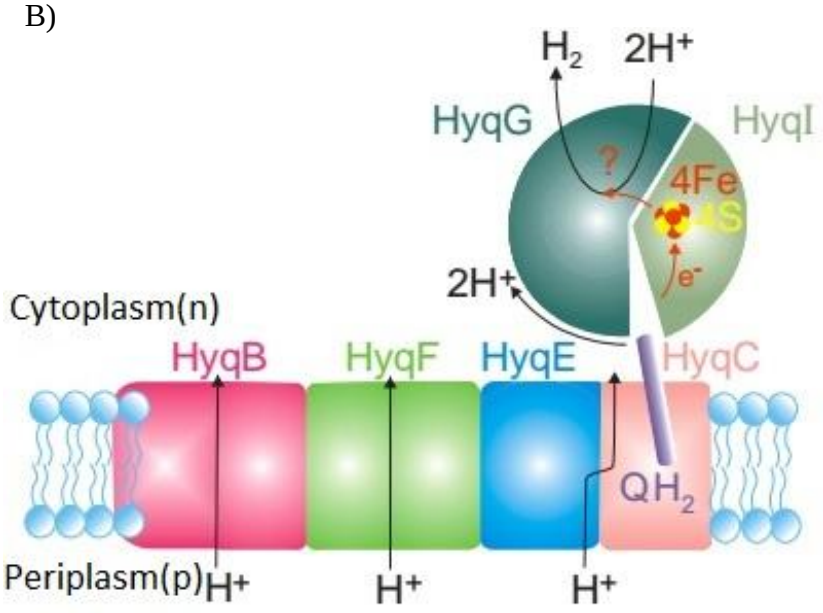

C)

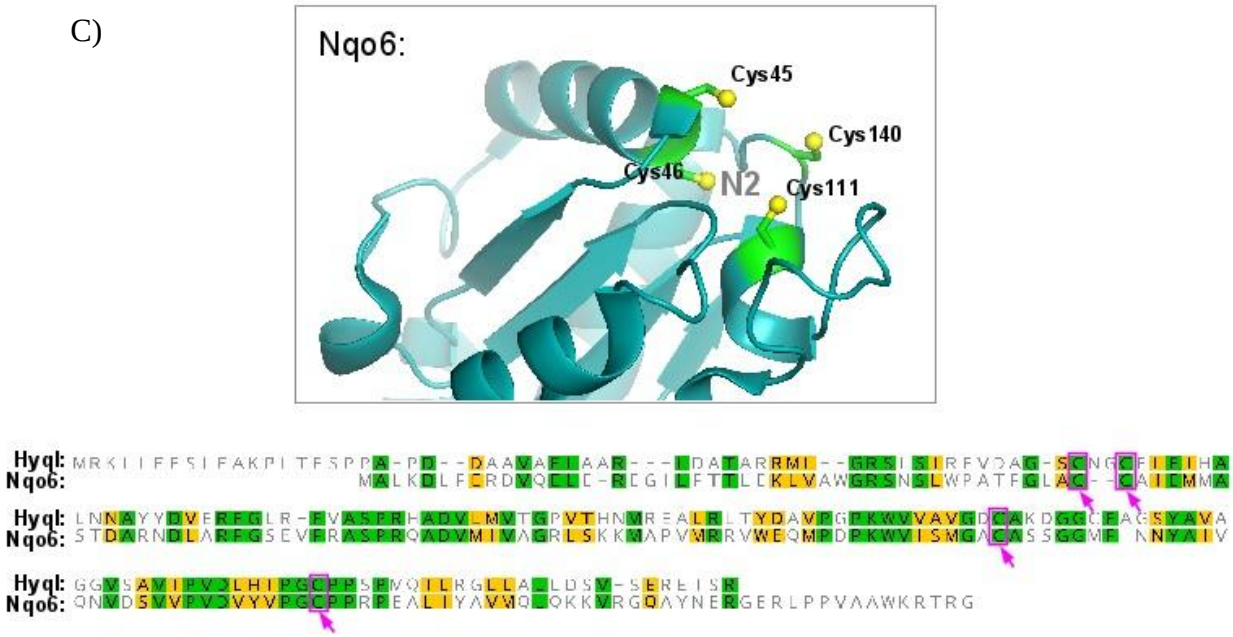

Fig 4: (A) Crystal structure (ribbon) of NADH:ubiquinone oxioreductase of *Thermus thermophilus* **[17]**. (**B**) Cartoon diagram of the proposed structure of the hyq hydrogenase, HyqG(Nqo5:4),HyqI (Nqo6) and 4Fe4S center (N2), HyqC(Nqo8), HyqE (Nqo10), HyqF(Nqo13), HyqB(Nqo12). HyqG is uncharacterized. **(C)** Protein sequence alignment of Nqo6 and HyqI showing the positions of the conserved Cys residues.

Photo-hydrogenic Micro-organisms

Although hydrogenic enzymes exist in many different types of micro-organisms, the metabolic system of the organism is a critical factor to consider for sustained high rates of H_2 production. Therefore, photo-hydrogenic micro-organisms such as cyanobacteria and algae have been extensively studied because they are equipped with oxygenic photosynthesis, which offers the unique capability of oxidizing H_2O as an electron source. Through the course of 3.5Gyrs of evolution **[19]**, contemporary photo reaction centers have evolved to convert captured light energy into chemical energy

with extraordinary efficiency **[20]**. In oxygenic photosynthetic organisms that also produce H_2, electrons oxidized from water are excited by light to a high energy state capable of driving dinitrogenase and/or hydrogenase based H_2 production **[4]**. However, the oxidation of water $2H_2O + 8hv \rightarrow 4H^+ + O_2 + 4e^-$ inevitably produce O_2, a potent inhibitor of known hydrogenic enzymes **[4]**. Although the oxygen evolving water splitting complex of oxygenic photosynthesis can obtain cheap and abundant electrons from H_2O, it remains a critical obstacle in establishing oxygenic phototrophs as a suitable vector for H_2 production **[4]**.

However, some organisms have a different, more ancient type of photosynthetic metabolism called anoxygenic photosynthesis. Anoxygenic photosynthesis predates the evolutionary development of the water splitting complex and therefore does not oxidize H_2O as an electron source. Instead of H_2O, anoxygenic phototrophs use a wide set of organic and inorganic electron donors to run their cellular processes. Of relevance to this study is the purple non-sulfur bacterium *Rhodopseudomonas palustris* (*R.palustris*) an anoxygenic phototroph with a wide metabolic versatility and the ability to produce H_2 **[21]**.

Rhodopseudomonas Palustris

R.palustris is an α-*Proteobacteria* diazotroph, able to use N_2 as the sole nitrogen source **[21]**. They are commonly found in environments such as swine-waste lagoons, earthworm droppings, pond water, and marine coastal

settings. Of interest to many researchers is the extreme metabolic versatility of *R.palustris*, consisting of four main metabolic modes.

- Chemoheterotroph: Electrons and carbons obtained from organic compounds (White colonies)
- Chemoautotroph: Electrons and carbons obtained from inorganic compounds (White colonies)
- Photoheterotroph: Electrons and carbons obtained from organic compounds with the aid of light (Dark purple colonies)
- Photoautotroph: Electrons and carbons obtained from inorganic compounds with the aid of light (Dark purple colonies)

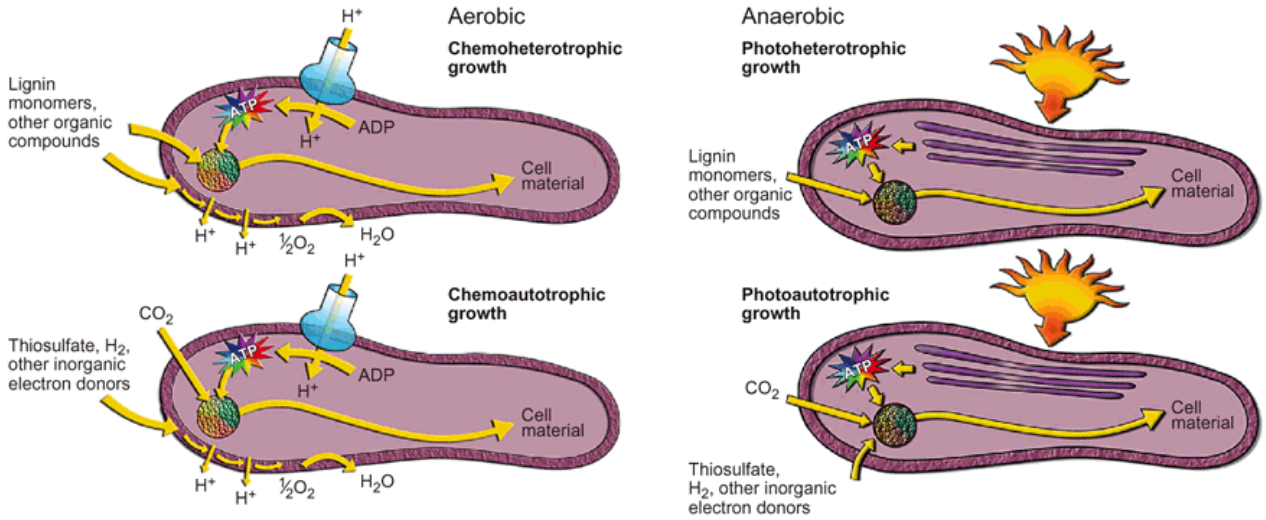

Fig 5: The four main metabolic modes of *R.palustris* **[22]**

Under aerobic conditions, *R.palustris* colonies are opaque with no detectable photopigments and default to oxidative phosphorylation. When O_2 becomes limiting and sufficient light is provided, *R.palustris* colonies will produce purple photopigments and resort to cyclic phosphorylation **[23,24].** The photosystem core complex uses light energy to push low chemical energy electrons from the periplasmic cytc2 pool to the membrane quinone pool. In turn, photosynthetic membrane quinol will drive cytbc1 complex activity, generating a proton gradient in the process and returning the electrons to the cytc2 pool **[4, 21]**. Therefore, cyclic phosphorylation activity continuously excites low chemical potential electrons oxidized from cytc2 to a high chemical potential to drive cellular processes. From a thermodynamics standpoint, exogenous electron donors able to reduce cytc2 can be used to produce H_2. Like *A. caulinodans,* some strains of *R.palustris* possess the *hyqBCEFGI* operon. Therein, we set out to characterize the previously identified *hyq* from the non-photosynthetic A. caulinodans in the anoxygenic photosynthetic *R. palustris*.

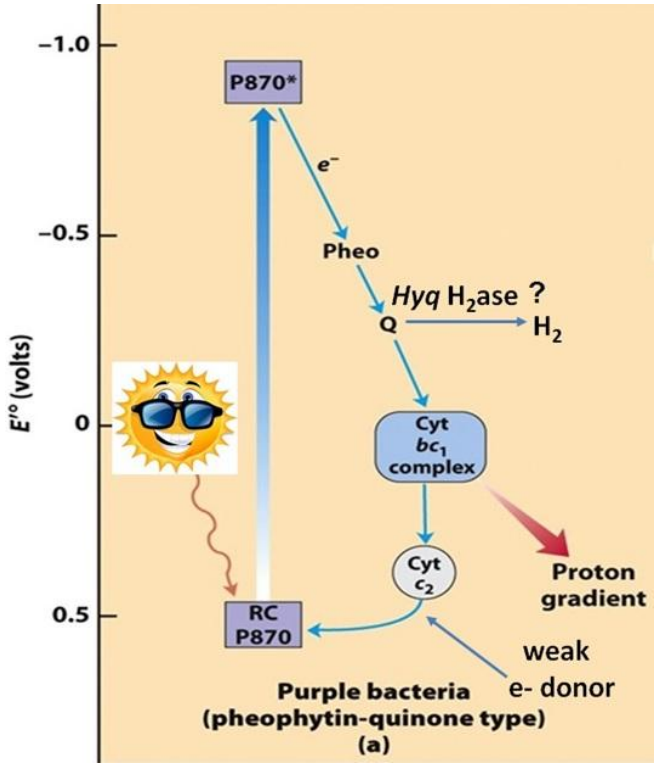

Fig 6: Diagram of the electron pathway for purple bacteria during cyclic phosphorylation and the proposed Hyq hydrogenase[**25**].

Results, Materials, and Methods

Media

All strains were routinely grown in RP2.2 defined minimal media or in RP2.2C unless stated otherwise. The composition of RP2.2 is as follows: (10 m*M*) potassium succinate, (5 m*M*) potassium phosphate pH 6.3, (1.5 m*M*) ammonium bicarbonate (0.15 m*M*) sodium thiosulfate, (0.1 m*M*) magnesium sulfate (0.05 m*M*) calcium chloride, (15 µ*M*) *p*-aminobenzoate, (5 µ*M*) nicotinate, (1 µ*M*) ferric ammonium citrate, (1 µ*M*) *d*-biotin, (1 µ*M*) folate, and (0.1 µl/ml) Hutner's trace metals "44" in which (0.1 m*M*) sodium molybdate was substituted for iron sulfate. The composition of RP2.2C is the same as RP2.2 except potassium succinate was lowered to 2mM and 0.025% (w/v) casamino acid was added.

Rhodopseudomonas palustris HaA2

We examined the *R.palustris* genome of seven sequenced wild isolates by the VISTA [**26**] algorithm for the hup^+/hyp^+ operon encoding the membrane bound group I uptake hydrogenase **[12,27]**, as well as the unlinked, membrane integral hyq^+ locus encoding the group IV-like *hyq* hydrogenase **[12]**. All seven *R.palustris* wild isolates carry at least one locus, three isolates carry both locus, three isolates carry only the hup^+/hyp^+ locus, and one isolates carry only the unlinked hyq^+ locus. *R.palustris* HaA2 was chosen for further study because it's genotype was naturally hyq^+, Δ*hup/hyp*.

Both Hyq and Nif produce H_2 in HaA2 photo-induced liquid cultures.

While other sequenced strains of *R.palustris* may be anaerobically cultured in defined minimal media, HaA2 cannot. Therefore, to assess the H_2 production activity of phototrophic HaA2 liquid cultures, starter cultures were aerobically grown for 5 days and diluted 1:100 into 35ml serum vials filled 2/3 of the way with RP2.2 media. Inoculated culture vials were septum-sealed and placed on a shaker for 4 days at 29°C. After 4 days, sealed cultures would become O_2 limited and reach a static cell density, with viable cell counts of ~1.0×10^8 cells ml^{-1}. To induce photosynthesis (photo-induction), a sterile 25 gauge needle would be inserted in the septum of each arrested, heterotrophic culture. The exposed needle orifice was then plugged with sterile cotton, covered with surgical tape to prevent contamination from the external air, and placed into a 29°C incubator for an additional 3 days with a 60W incandescent light placed 15-20 cm away. Therein, viable cell counts increased to ~$3x10^8$ cells ml^{-1} and have newly produced photopigments. Photo-induced liquid cultures would become visibly purple and have a sharp increased absorbance at 880nm when measured by a spectrophotometer**[23]**. From experience, photopigments are visible by the unaided eye at an OD880/660 ratio of ~0.75 and higher ratios correlate with a darker purple color (Fig 7).

R.palustris HaA2 photo-induced culture vials were then sparged with N_2 gas for 25-30min at 60ml/min to establish a baseline H_2 concentration. The previously inserted needle was then removed and newly produced H_2 was allowed to accumulate inside the sealed vials. Internal H_2 concentrations were sampled using a gas tight syringe (Hamilton) and analyzed by gas chromatography (Peak Laboratories), with a HgO photometer, over the course of 24hrs. Within a ~24hr period, internal H_2 concentrations of photo-induced HaA2 increased by 256.4ppm (Fig 9A).

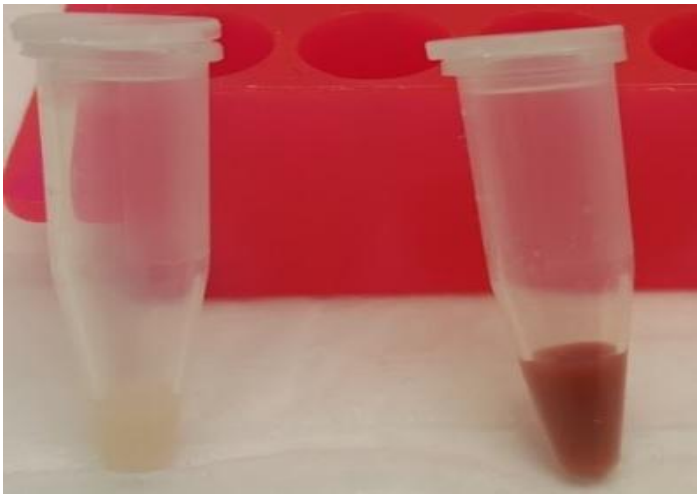

Fig 7: Spun down HaA2 cultures after 7 days of growth; (Left) Sealed for 7days with an OD880/660 <0.75, (Right) Sealed then pierced with 25 gauge needle at day 4 with an OD880/660 >0.75

To gain a qualitative understanding of the inferred involvement in the H_2 production activity of *hyq* and *nif*, total RNA was isolated with Trizol from a replicate photo-induced HaA2 culture. Gene expression levels of *hyq* and *nif* were assessed using reverse transcriptase PCR (RT-PCR).

Despite excess ammonium in the media, HaA2 photo-induced cultures continued to express *nif* at high levels, whereas the expression of *hyq* was barely detectable (Fig 8).

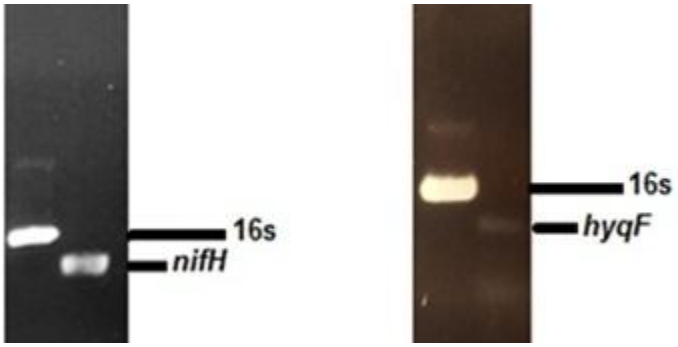

Fig 8: RT-PCR of *nif* and *hyq* from photo-induced HaA2.

To determine if *nif* and *hyq* are the sole producers of H_2 in HaA2 photo-induced liquid cultures, deletion mutants were constructed and analyzed for accumulated H_2 concentration as described earlier. Of the three known dinitrogenase complexes of diazotrophic bacteria, HaA2 only encodes for the Mo-dinitrogenase. Accordingly, we constructed a deletion mutant in which genes *nifH* through *nifQ* were removed. The resulting strain, HaA2-14 (Δ*nifHQ)*, carries a unique 21bp sequence in place of the 9.2kbp *nifH*$^+$-*nifQ*$^+$ locus, verifiable by PCR [**28,29**, Table 1] .In addition, both HaA2 and HaA2-14 (Δ*nifHQ*) strains were subjected to further deletion of the unlinked 7.1kbp *hyqBCEFGI*$^+$. Gene deletion mutants were again identified using a unique 21bp sequence in place of the *hyq*$^+$ operon, resulting in the single deletion mutant HaA2-51(Δ*hyqBI*) and the double

deletion mutant HaA2-56 (Δ*nifHQ,* Δ*hyqBI*, Table 1). In photo-induced HaA2-51 cultures, H_2 levels reached a concentration of 912ppm within a 24hr period. In contrast, measured H_2 concentration of photo-induced HaA2-14 and HaA-56 cultures reached 7.83ppm and 1.57ppm, respectively (Fig 9B-D). The *nifHQ*$^+$ strains displayed markedly higher H_2 concentrations than the Δ*nifHQ,* as expected given the much higher expression of *nif* compared to *hyq.* Although measured H_2 concentrations were two orders of magnitude higher in the *nifHQ*$^+$ strains than the Δ*nifHQ strains,* HaA2-14 nevertheless remained hydrogenic (Fig 9B,C).

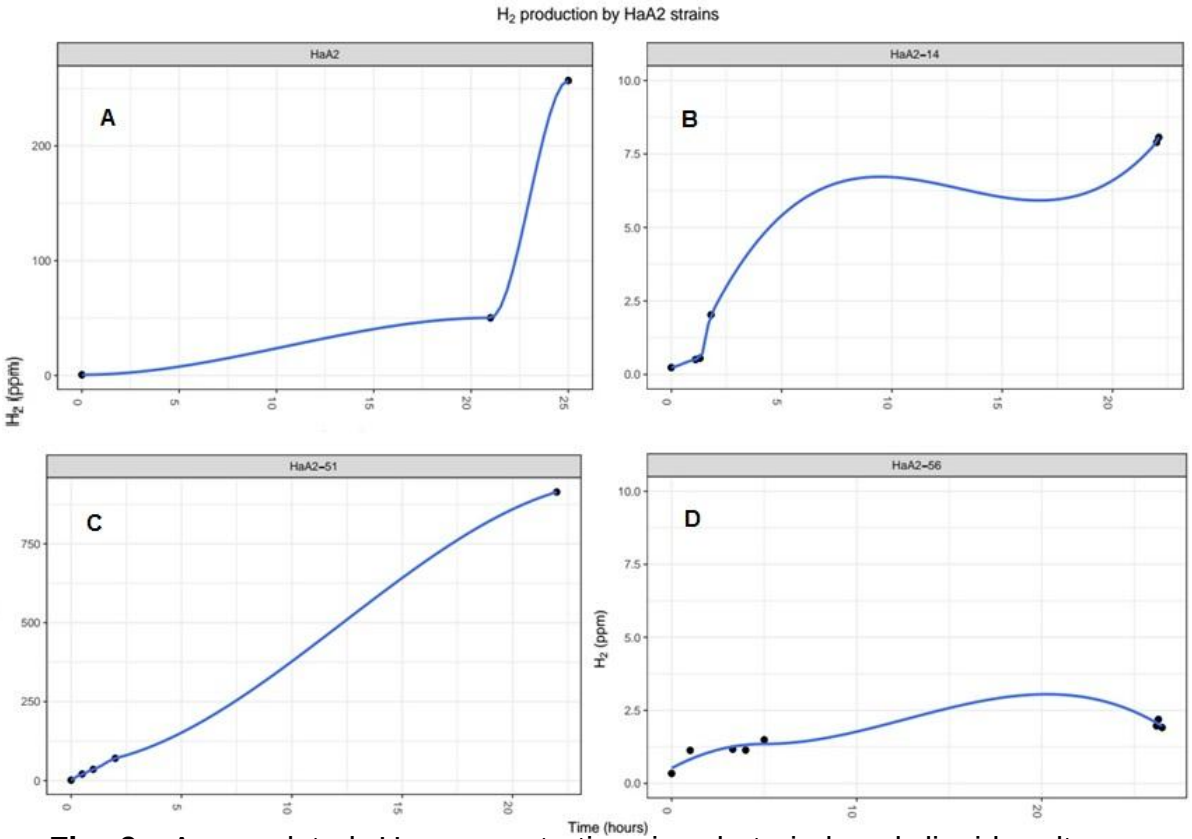

Fig 9: Accumulated H_2 concentration in photo-induced liquid cultures; **A)**HaA2, **B)**HaA2-14 (Δ*nifHQ)*, **C)**HaA2-51(Δ*hyqBI)*, **D)**HaA2-56 (Δ*hyqBI* ,Δ*nifHQ)*.

Bacterial Strain	Genotype
HaA2 wild type	*hyq*$^{+}$, *nif*HQ^{+}
HaA2-14	*hyq*$^{+}$, Δ*nifHQ*
HaA2-51	Δ*hyqBI*, *nif*HQ^{+}
HaA2-56	Δ*hyqBI* ,Δ*nifHQ*
HaA2-117	Hyq^{I} , *hyq*$^{+}$, Δ*nifHQ*,

Table 1: HaA2 and its derivatives with respective genotypes shown.

H_2 production cannot be driven by thiosulfate

Next, H_2 production was assessed using the inorganic electron donor thiosulfate. HaA2 carries a locus encoding fifteen subunits of a highly conserved α-Proteobacterial sulfur oxidase (Sox) complex. The periplasmic Sox complex catalyzes an 8 e^{-} oxidation of thiosulfate and reduces cytc2 as the final electron acceptor **[30, 31]**. In addition, photo-induction of *R.palustris* involves the synthesis of intracytoplasmic photosynthetic membrane (ICM), where the lumen is contiguous with the perisplasm **[32].** Therefore, the H^{+} released from the oxidation of thiosulfate by the Sox complex directly contributes to the ICM proton-motive force and the reduced cytc2 is oxidized by the photo reaction center to run cyclic phosphorylation **[30].**

The previous photo-induction method was modified in order to monitor OD660 growth in balch tubes. As mentioned before, other sequenced *R.palustris* strains have been shown to grow under anaerobic

condition in defined media, whereas HaA2 cannot (Fig 10A). However, with the addition of 0.025% (w/v) Casamino acid to the RP2.2 media, HaA2 can grow photoheterotrophically. The modified culturing technique provided a simpler approach to track growth differences between +/- thiosulfate samples. Therefore, future photoheterotrophic growth conditions used RP2.2C, which shares the same composition as RP2.2 except for the reduction of potassium succinate concentration to 2mM and the addition of 0.025% (w/v) casamino acid.

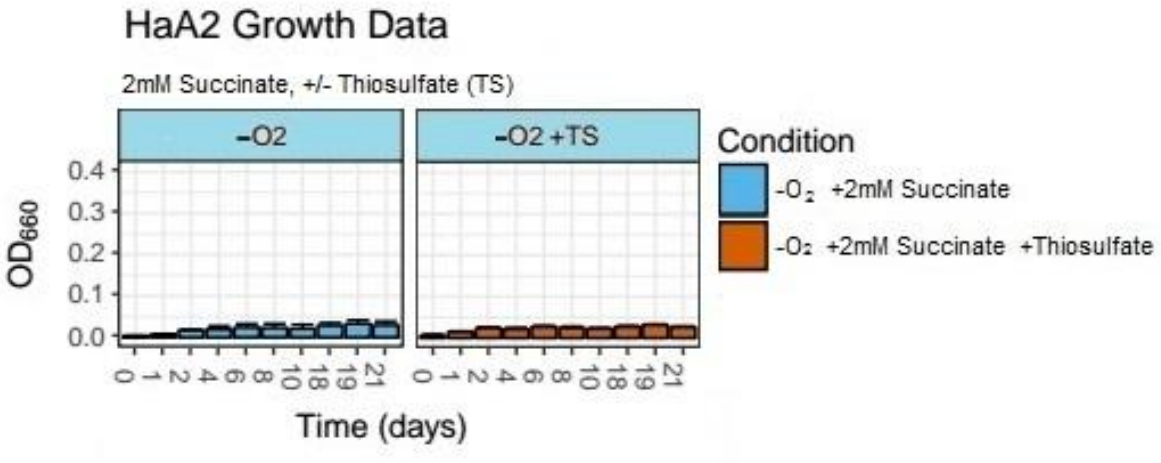

Fig10: OD660 of HaA2 in defined media

Thereafter, thiosulfate oxidation activity was indirectly assessed through standard growth curve of HaA2 in RP2.2C +/- 3mM sodium thiosulfate. HaA2 starter cultures were diluted 1:100 into N_2 sparged RP2.2C +/- 3mM sodium thiosulfate**.** After 2 weeks of incubation, OD660 readings of HaA2 cultures with added sodium thiosulfate reached 0.579 vs 0.305 without sodium thiosulfate (Fig 11A). HaA2 was also tested for

photoautotrophic growth using thiosulfate as the e^- donor. In the photoautotrophic version of RP2.2C media, where 2mM potassium succinate and 1.5mM ammonium bicarbonate were replaced by 2.25mM sodium thiosulfate, 0.75mM ammonium thiosulfate, and 15mM sodium bicarbonate. In two trials an additional 0.025% (w/v) casamino acid was added. Starter cultures were diluted 1:100 into N_2 sparged photoautotrophic media, standard RP2.2C, and RP2.2C (absent of electron donors), the latter two conditions served as controls. Despite having a positive effect on photoheterotrophic growth, 3mM thiosulfate did not sustain photoautotrophic growth **(Fig 11B).**

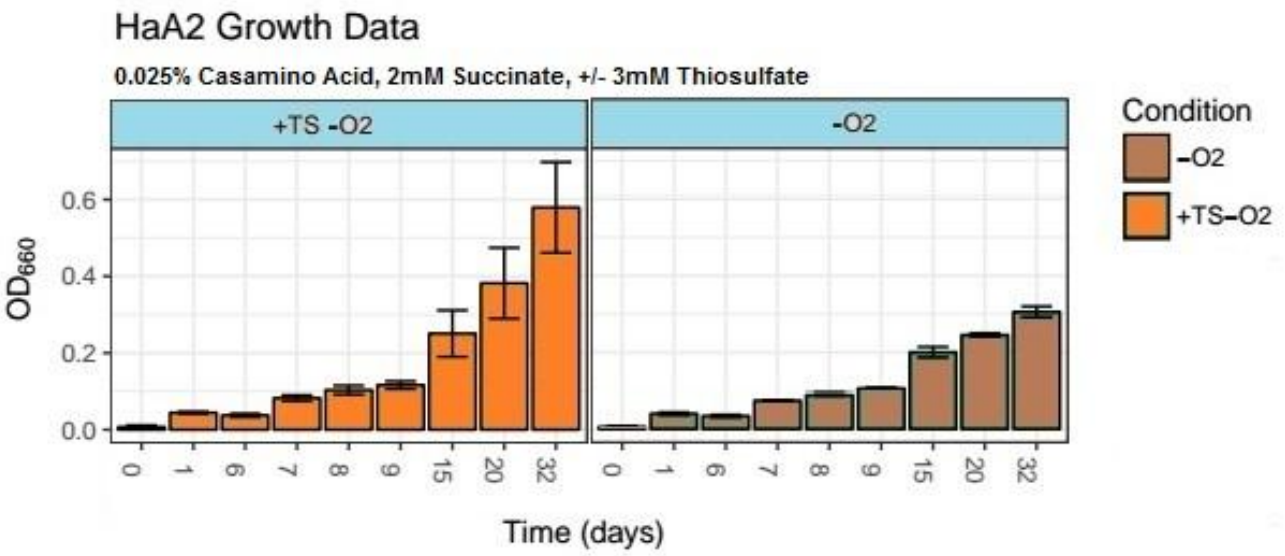

11A: OD660 of HaA2 in defined media +0.025%Casamino acid, +/- 3mM thiosulfate

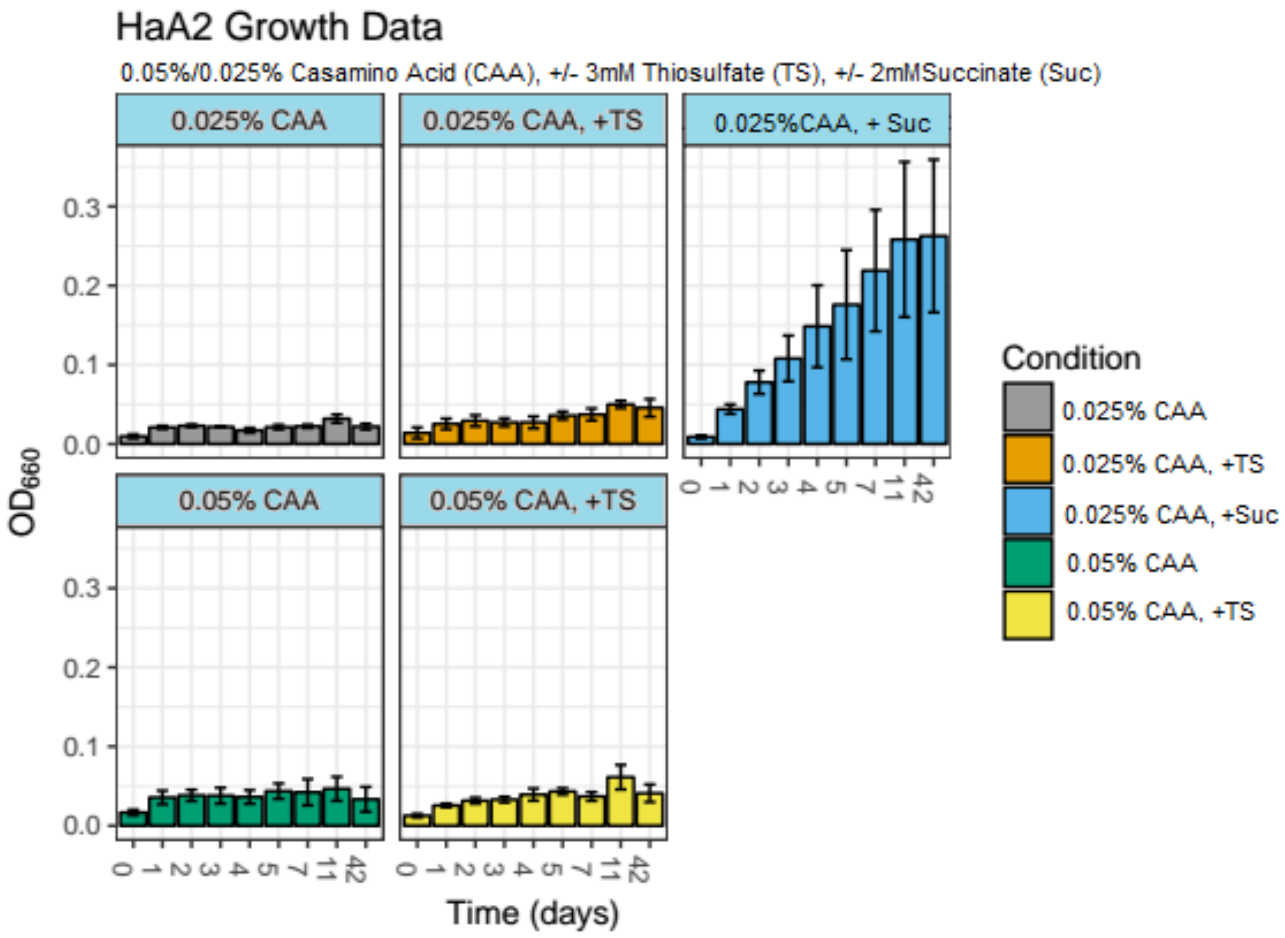

Fig11B: OD660 of HaA2 in photoautotrophic conditions

Since thiosulfate dependent H_2 production could not be tested in photoautotrophic cultures, HaA2 was photoheterotrophically grown in RP2.2C, washed and suspended in 10mM phosphate buffer pH= 6.3. Starter cultures were again diluted 1:100 into 120ml serum vials filled to the top with RP2.2C, crimp sealed, and placed in a 29°C growth chamber incandescent light supplied by a 60W light bulb for 10 days. Photoheterotrophic cultures were then spun down, washed, and suspended in 10mM phosphate buffer

pH=6.3. The original 120ml was concentrated into 60mls of phosphate buffer and distributed evenly among 6 balch tubes and crimp sealed. All steps, besides the centrifugation, were carried out in an anaerobic chamber. Subsequently, all six culture tubes were sparged with N_2 to reduce carry over H_2 from the anaerobic chamber. OD660 and OD880 measurements were taken to assure equal distribution of cells and to assess intensity of photopigments. Suspended cultures shared an OD660 of 0.45 and an OD880 of 0.59 for an OD880/600 ratio of 1.31. After the initial gas sample, 3mM of sodium thiosulfate was added to three of the six culture tubes and all six culture tubes were placed back into the 29°C growth chamber. Over the course of 24 hours, H_2 concentrations were sampled as described earlier. In HaA2 washed and suspended cultures, the addition of thiosulfate did not produce higher amounts of H_2 compared to control. Apart from an initial H_2 concentration increase, perhaps from the oxidation of stored poly-hydroxy-butyrate, H_2 levels were comparable for all samples.

(Fig 12).

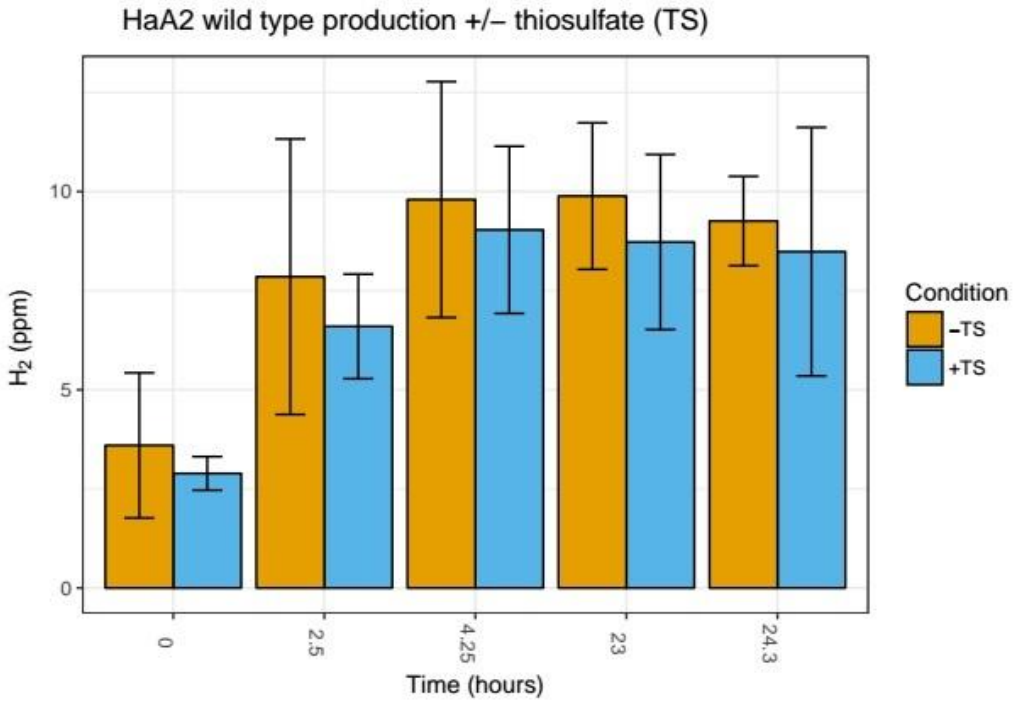

Fig 12: Accumulated H_2 concentration for HaA2+/- 3mM sodium thiosulfate.

To test if succinate could drive H_2 production, four culture tubes, HaA2 # 1-4, from the previous suspension assay were chosen for subsequent testing. Succinate was added to HaA2 # 1 and #4 at a final concentration of 8.5 mM from a N_2 sparged stock (Fig 13). One milliliter of air was injected into HaA2 #1 to test if micro amounts of O_2 would be conducive to H_2 production (a theory of my late PI). HaA2 #2 and HaA2 #3 served as controls, the former contained 3mM sodium thiosulfate from the previous experiment and the latter received 3mM sodium thiosulfate during this experiment. All samples contained equal concentrations of sodium thiosulfate. H_2 levels were sampled after 8 days.

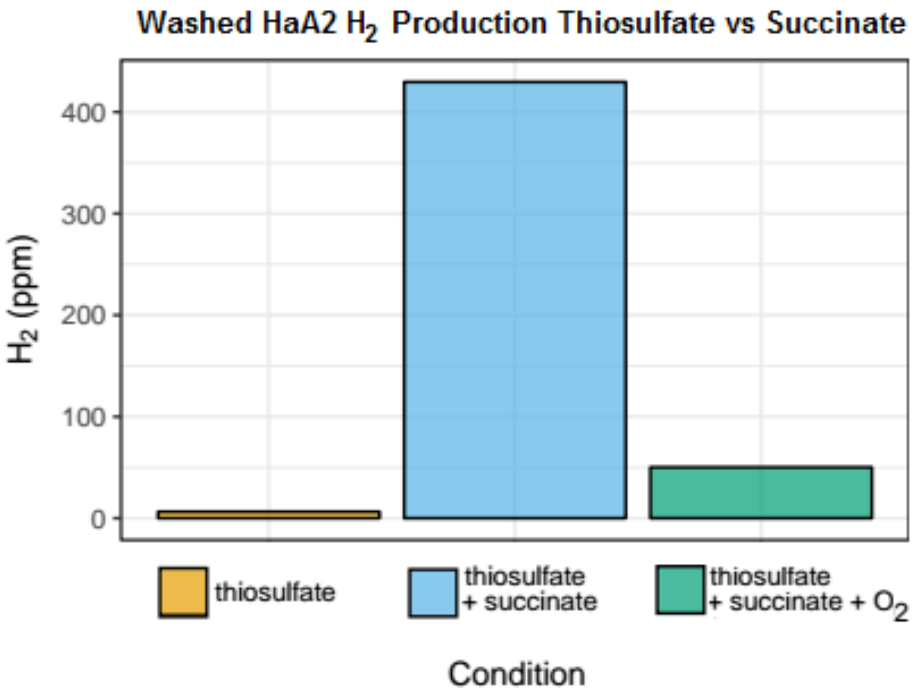

Fig 13: Accumulated H_2 concentration for washed HaA2 +/- succinate**.**

HaA2 #1 produced ~5 times higher amounts of H_2 when compared to HaA2 #2 and #3 but was ~9 fold less than HaA2 #4. HaA2 #2 and #3 did not show signs of H_2 production. Accumulated H_2 in HaA2 #4 was 2 orders of magnitude higher than the washed cultures containing only sodium thiosulfate and ~9 time higher than succinate plus micro amounts of O_2. Thus, H_2 production in washed then suspended HaA2 cultures is driven by succinate oxidation and is more active in an anaerobic vs micro-aerobic environment. Despite aiding in photoheterotrophic growth, sodium thiosulfate dependent H_2 production was not detected.

***Endogenous hyq promoter replaced by Ps. putida* NahR activator *in cis* with its P*nahG* promoter.**

From our previous RT-PCR analysis of photo-induced HaA2 cultures, we detected faint transcription levels of *hyq*. Accordingly, we proceeded to replace the endogenous *hyq*$^{+}$ operon promoter in the HaA2-14 bacterial strain with a salicylate inducible NahR transcriptional activator, from *Pseudomonas putida,* oriented *in cis* with its P*nahG* promoter **[34]**. The resulting mutant strain HaA2-117(Hyq^{I}, Δ*nifHQ)*, carries a novel *nahR*$^{+}$ P*nahG*::*hyq*$^{+}$ construct (Fig. 14, Table 1)

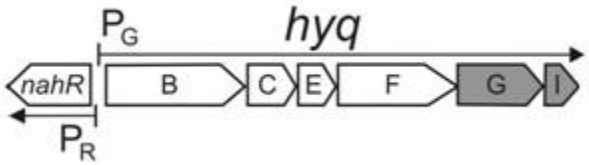

Fig 14: Position of the nahR activator in the nahR^{+}PnahG::hyq^{+} engineered construct

R.palustris HaA2-117 carrying the novel, engineered *hyq*$^{+}$ operon promoter regions was constructed by a modified “crossover” PCR method **[*29*]**. Wild isolate HaA2 genomic DNA was extracted and used as the template in two PCR amplifications with primer pairs: HyqA + HyqB-bar (AB) and HyqC-bar + HyqD (CD). The two ~1kbp PCR products were used in separate blunt end

molecular cloning reactions with pJET1.2/blunt as plasmid vector. Resulting recombinant plasmids were purified and analyzed by restriction double digest for proper orientation relative to the pJET1.2/blunt plasmid. The pHaA2hyqAB and pHaA2hyqCD DNA fragments were gel purified, mixed, annealed, and re-ligated using standard molecular cloning techniques. The recombinant product, plasmid pHaA2hyqAD carries two HaA2 genomic DNA segments from which the 428 bp HaA2 *hyq* operon promoter had been replaced with a synthetic 21 bp sequence that serves as a GAGCTC *Sac I* cleavage site and a verifiable sequence used to identify recombinant mutants. A replacement promoter sequence, a 1.4 kbp *nahR*(c)–P*nahR*(c)–P*nahG* DNA fragment was PCR amplified from the genome of *Pseudomonas putida* Nah7 that is able to catabolize salicylate. The 1.4 kbp DNA fragment was blunt-end cloned into pJET1.2/blunt and the resulting plasmid, pNahRG1347, was digested and the excised insert was annealed with linearized pHaA2hyqAD. The resulting 6.7 kbp recombinant plasmid was analyzed for the desired orientation of the *nahR*(c)–P*nahR*(c)–P*nahG* insertion at the *in vitro* ΔP*hyq* locus by restriction digest gel electrophoresis. Recombinant plasmid, pHaA2hyqAD3N, carrying the *in vitro* engineered *hyq* promoter region was confirmed by DNA sequencing.

Preparatory to recombination in *R.palustris* strains, the 3.7 kbp insert DNA fragment of pHaA2hyqD3N was cloned into plasmid pJQ200SK (Table 3). The 5.3kbp pJQ200SK was digested with restriction enzymes and gel

purified. Likewise, purified pHaA2hyqAD3N was digested for the 3.7 kbp insert fragment and purified by gel electrophoresis. The 5.3 kbp and 3.7 kbp DNA fragments were annealed and ligated with T4 DNA ligase. The resulting recombinant plasmid was analyzed again by double digestion and sequenced to confirm the 9.0 kbp recombinant plasmid pJQhyqAD3N. All other recombinant DNA template constructions and gene replacements were carried out in a similar manner. All PCR primer sets can be found in Table 2.

Recombinant plasmid pJQhyqAD3N was electroporated into *E.coli* S-17 followed by conjugation of S-17/pJQhyqAD3N with HaA2 on agar plates containing (10m*M*) potassium succinate, (5m*M*) potassium phosphate pH 6.3, 0.1% (w/v) salt-free casamino acids, 0.05% (w/v) yeast extract, and 0.2% (w/v) D-glucose. Recombinant candidates were selected on RP2.2 plates with added (250ug/ml) gentamicin. Single colonies were again selected and struck out onto RP2.2 agar plates plus 250ug/ml gentamicin to confirm Gm^R. Single colony candidates were then selected and struck onto RP2.2 non selective plates. After 5-7 days of incubation at 30°C, true recombinants were confirmed by colony PCR using PCR primers at both ~1 kbp proximal and ~1 kbp distal to the genomic homologous integration site and a synthetic 21bp sequence (Table2).

From non-selective RP2.2 plates, confirmed single colony candidates were selected and struck onto RP2.2 + 10% sucrose plates, selecting for double recombinants. Early growing sucrose-resistant colonies were tested

for Gm^R by patching onto RP2.2 plates supplemented with gentamicin (250 µg/ml) and 10% sucrose. Sucrose resistant but Gm^S colonies were propagated non-selectively on RP2.2 plates and analyzed further. To distinguish between reverted wild type and gene replacement derivatives, the same two PCR tests as previously described were used to verify recombinants. Null amplification from both proximal and distal ~1 kbp PCR products is evidence of reconstituted wild type, whereas the presence of both ~ 1 kbp PCR products is evidence of gene-replacement derivatives. Identified mutants each carried the signature locus with its unique 21 bp sequence. HaA2 wild-type and HaA2-95 were tested in aerobic and microaerobic phototrophic liquid batch cultures for the ability to take up (50 µ*M*) [^{14}C]salicylate, the NahR inducer. Both strains accumulated salicylate at similar rates; both strains failed to photo-oxidize salicylate in micro-aerobic cultures (Personal communication with Bob Ludwig).

R. palustris HaA2	*hyq* locus	
HaA2-1440203	Hyqprox2	CGCCACCAACGAGAAGAGCA
HaA2-1440244	Hyqprox	GCGAATACAAGGCCAAGCAC
HaA2-1440309	HyqA	GTTGCAGACCCGCACCAAGAG
HaA2-1441350C	HyqB+bar	GTCAACTGCGACCTTGGCCACTGCTCAGCCAGGTC*GAGCTC*
HaA2-1441778	HyqC+bar	CTGCTCAGCCAGGTC*GAGCTC*ATGACTGAACTTGCGGTTCAG
	hyq "barcode"	CTGCTCAGCCAGGTC*GAGCTC*
HaA2-1443033C	HyqD	AGTTGCGGGCTCTGCAGCA
HaA2-1443133C	Hyqdist	ACGCCATAGGCCTTGACGAA

HaA2-1448969	HyqtermC+bar	CTGCTCAGCCAGGTC*GAGCTC*CGCGCGACTAATGACTGGTG
HaA2-1149957C	HyqtermD	CGTACATCGCCGGGTTCTC
HaA2-1450079C	Hyqtermdist	GGTCGGATGCACCGAGTTTTCA
Ps putida nah locus		
	NahR-stopC	CATGAAAGACAGGACACCGTTC
	NahG-start	CAAGTCATCAATAAAGCCATCACGA
Nah7-43158		AAAA*GAGCTC*GGAACGGTGTCCTGTCTTTCATGG
Nah7-44485C		AAAA*GAGCTC*GTCGTGATGGCTTTATTGATGACTTGTTAA
R. palustris HaA2	*nif* locus	
HaA2-1114139	Nifprox	CGCCGGCCGCGAATTATCTG
HaA2-1114184	NifA	TCCTGACCGAGATCGACATCC
HaA2-1115239C	NifB+bar	*GCCGAATTCGAGCGAGAGGCA*AAGTGCCGCCATGTTTTCTCTCC
HaA2-1124420	NifC+bar	*TGCCTCTCGCTCGAATTCGGC*GGCGTGGCGTGAGGACC
	nif "barcode"	*TGCCTCTCGCTCGAATTCGGC*
HaA2-1125566C	NifD	GGACGTGATCGCCGTCTGTA
HaA2-1125707C	Nifdist	CGCCTTGGTGTAGTGGGTCA

Table 2: Synthetic oligodeoxynucleotide PCR primers

HaA2-117 H_2 measurement

HaA2-117 (Hyq^{I}, Δ*nifHQ)*, carrying the engineered promoter, was grown and tested for H_2 production activity as described earlier. After confirming that the H_2 production activity in HaA2-117 was phenotypically equivalent to HaA2-56, 50uM of salicylate was injected into the culture vials using the Hungate method **[33]** and placed back in the 29^{o}C growth chamber. After ~20 hrs, accumulated H_2 levels were sampled (Fig 15**)**.

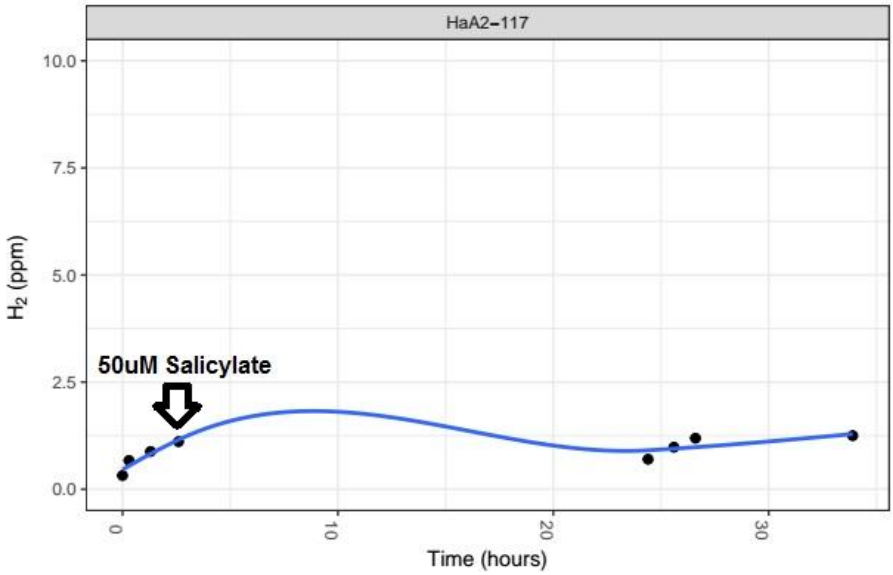

Fig 15: Accumulated H_2 concentration for HaA2-117 with salicylate inducer.

Surprisingly, accumulated H_2 in HaA2-117 only reached 0.93ppm, similar to HaA2-56. H_2 production pattern remained unchanged for supplemented sodium salicylate concentrations of 10, 50, and 100uM. To test for *hyq* gene expression, four replicate HaA2-117 photoheterotrophic cultures were grown for 10 days and then supplemented with 0, 10, 50, and 100uM of sodium

salicylate. After 24 hours, total RNA was isolated using Trizol and the *hyq expression* was probed using RT-PCR. Samples for all salicylate concentrations lacked detectable *hyq* expression **(Fig 16)**.

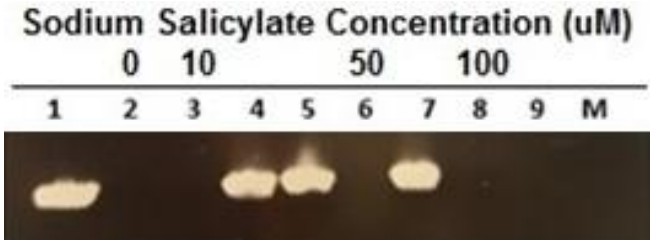

Fig 16: RT-PCR of HaA2-117 supplemented with 0, 10uM, 50uM, and 100uM sodium salicylate. 16s rRNA gene=lanes 1, 4, 5, and 7. *hyqF= lanes* 2, 3, 6, and 8.

Conclusion

Historically, the H_2 production activity of purple non-sulfur bacteria has been solely credited to the dinitrogenase complex activity **[4]**. While my results ostensibly agree with the body of literature, we have identified a second H_2 producing enzyme in the purple non-sulfur bacterium *R.palustris* HaA2. In our single deletion mutants (HaA2-14 and HaA2-51), both Nif and Hyq produced measurable amounts of H_2 above background levels. Although HaA2-51 produced significantly higher amounts of H_2 than HaA2-14 in a 24hr period, this difference is likely attributed to the pronounced higher expression of *nif* compared to *hyq*. Unfortunately, our attempt to induce the expression of *hyq* by replacing the endogenous *hyq* promoter with a salicylic acid inducible promoter, *nahR*$^{+}$P*nahG*::*hyq*$^{+}$, did not elicit the effect we anticipated. Nevertheless, despite faint transcription levels, we have shown that the previously observed H_2 production activity of *hyq* in *Azorhizobium caulinodans* [**16**] is shared in *R.palustris* HaA2. However, further work remains to be done to definitely prove that this effect is a light driven process in *R.palustris*.

While the sum total of H_2 produced in HaA2 photoheterotrophic cultures is largely due to Nif, Hyq has the potential to produce significantly greater amounts of H_2 than Nif. From the perspective of catalytic turnover, the Mo-dinitrogenase complex has a turnover rate of 5 s^{-1} [**7**], whereas the group IV Ni-Fe hydrogenase has a turnover rate of 1,000 s^{-1}[**3**]. If *hyq* was

expressed at the same level as *nif* under photoheterotrophic conditions, then H_2 concentrations could presumably reach 182,400 ppm within a 24hr period (912ppm from HaA2-51 x 200). Furthermore, taking into consideration the e^- requirement between the two enzyme complexes, the direct reduction of protons into H_2 by group IV Ni-Fe hydrogenases requires 75% less e^- than the reaction carried out by Nif. Therefore, H_2 production by Hyq is faster than Nif and can obtain 4 times as much H_2 per mole of electron donor.

Although photoautotrophic growth for *R.palustris* strain CGA009 has been demonstrated **[8]**, HaA2 did not grow photoautotrophically with 3mM thiosulfate and bicarbonate as the sole e^- and carbon source under pure N_2 head space. Perhaps replacing the pure N_2 headspace with a 5%CO_2/ bal N_2 head space will provide sufficient CO_2 concentration for optimal Rubisco activity. In addition, thiosulfate dependent H_2 production was not detected in washed and suspended HaA2 photoheterotrophic cultures. Again, this is contrary to the report from Harwood *et al*, where they demonstrated thiosulfate dependent H_2 production from dinitrogenase using non-growing CGA009 under an argon head space **[8]**.

References

1.Cook, J., Oreskes, N., Doran, P. *et al*. (2016). Consensus on consensus: a synthesis of consensus estimates on human-caused global warming. *Environmental Research Letters,11*(4), 048002.

2. Tsao, J., Lewis, N., Crabtree, G. (2006). Solar FAQs. Retrieved from May 1, 2017 http://www.sandia.gov/~jytsao/Solar%20FAQs.pdf

3. Shafaat, H. S., Rüdiger, O., Ogata, H., & Lubitz, W. (2013). [NiFe] hydrogenases: A common active site for hydrogen metabolism under diverse conditions. *Biochimica et Biophysica Acta (BBA) - Bioenergetics,1827*(8-9), 986-1002.

4. S. Venkata Mohan and Ashok Pandey, Chapter 1 - Biohydrogen Production: An Introduction, In Biohydrogen, Elsevier, Amsterdam, 2013, Pages 1-24.

5. Philippe Constant and Patrick C. Hallenbeck, Chapter 5 - Hydrogenase, In Biohydrogen, edited by Ashok Pandey, Jo-Shu Chang, Patrick C. Hallenbecka and Christian Larroche, Elsevier, Amsterdam, 2013, Pages 75-102.

6. Joerger R, Bishop PE (1988) Bacterial alternative nitrogen fixation systems. *CRC Crit*

7. Thorneley RNF, Lowe DJ (1985) in *Molybdenum enzymes*; Spiro, T G, Ed; Wiley-Interscience: New York, pp 221-284.

8. Huang, J. J., Heiniger, E. K., Mckinlay, J. B., & Harwood, C. S. (2010). Production of Hydrogen Gas from Light and the Inorganic Electron Donor Thiosulfate by Rhodopseudomonas palustris. *Applied and Environmental Microbiology,76*(23), 7717-7722.

9. Hillmer, P., and H. Gest. (1977). H_2 metabolism in photosynthetic bacterium *Rhodopseudomonas capsulata*: H_2 production by growing cultures.J. Bacteriol. 129:724-731.

10. Fixen, Kathryn R., Yanning Zheng, Derek F. Harris, Sudipta Shaw, Zhi-Yong Yang, Dennis R. Dean, Lance C. Seefeldt, and Caroline S. Harwood. (2016). Light-driven carbon dioxide reduction to methane by nitrogenase in a

photosynthetic bacterium. *Proceedings of the National Academy of Sciences* 113.36: 10163-0167.

11. Thiel, T. (n.d.). Nitrogen Fixation in Heterocyst-Forming Cyanobacteria. *Genetics and Regulation of Nitrogen Fixation in Free-Living Bacteria Nitrogen Fixation: Origins, Applications, and Research Progress,* 73-110.

12.Vignais PM, Billoud B, Meyer J (2001) Classification and phylogeny of hydrogenases. *FEMS Microbiol Rev* 25: 455-501.

13. Lubitz, W., Ogata, H., Rüdiger, O., & Reijerse, E. (2014). Hydrogenases. *Chemical Reviews,114*(8), 4081-4148.

14. Ng, G., Tom, C. G., Park, A. S., Zenad, L., & Ludwig, R. A. (2009). A Novel Endo-Hydrogenase Activity Recycles Hydrogen Produced by Nitrogen Fixation. *PLoS ONE,4*(3).

15. Ciccolella, C. O., Raynard, N. A., Mei, J. H., Church, D. C., & Ludwig, R. A. (2010). Symbiotic Legume Nodules Employ Both Rhizobial Exo- and Endo-Hydrogenases to Recycle Hydrogen Produced by Nitrogen Fixation. *PLoS ONE,5*(8).

16. Sprecher, B. N., Gittings, M. E., & Ludwig, R. A. (2012). Respiratory Membrane endo-Hydrogenase Activity in the Microaerophile Azorhizobium caulinodans Is Bidirectional. *PLoS ONE,7*(5).

17. Baradaran R, Berrisford JM, Minhas GS, Sazanov LA (2013) Crystal structure of the entire respiratory complex I. *Nature* 494: 443-448.

18. Efremov, R. G., & Sazanov, L. A. (2012). The coupling mechanism of respiratory complex I — A structural and evolutionary perspective. *Biochimica et Biophysica Acta (BBA) - Bioenergetics,1817*(10), 1785-1795.

19. Des Marais DJ. (2000) Evolution: When did photosynthesis emerge on Earth? Science 289: 1703–1705

20. Yaghoubi, H., Lafalce, E., Jun, D., Jiang, X., Beatty, J. T., & Takshi, A. (2015). Large Photocurrent Response and External Quantum Efficiency in Biophotoelectrochemical Cells Incorporating Reaction Center Plus Light Harvesting Complexes. *Biomacromolecules,16*(4), 1112-1118.

21. Basak, N., & Das, D. (2006). The Prospect of Purple Non-Sulfur (PNS) Photosynthetic Bacteria for Hydrogen Production: The Present State of the Art. *World Journal of Microbiology and Biotechnology,23*(1), 31-42.

22. Larimer, F. W., Chain, P., Hauser, L., *et al*. (2003). Complete genome sequence of the metabolically versatile photosynthetic bacterium Rhodopseudomonas palustris. *Nature Biotechnology,22*(1), 55-61.

23. Scheuring S, Goncalves RP, Prima V, Sturgis JN (2005) The photosynthetic apparatus of *Rhodopseudomonas palustris*: structures and organization. *J Mol Biol* 358: 83-96.

24. Braatsch, S., Johnson, J. A., Noll, K., & Beatty, J. T. (2007). The O2-responsive repressor PpsR2 but not PpsR1 transduces a light signal sensed by the BphP1 phytochrome inRhodopseudomonas palustrisCGA009. *FEMS Microbiology Letters,272*(1), 60-64.

25. Lehninger, A. L., Nelson, D. L., & Cox, M. M. (2000). *Lehninger principles of biochemistry*. New York: Worth Publishers.

26. Frazer KA, Pachter L, Poliakov A, Rubin EM, Dubchak I (2004) VISTA: computational tools for comparative genomics. *Nucleic Acids Res* 32: 273-279.

27. Oda Y, Larimer FW, Chain PS, Malfatti S, Shin MV, Vergez LM, Hauser L, Braatsch S, Beatty JT, Pelletier DA, Schaefer AL, Harwood CS (2008) Multiple genome sequences reveal adaptations of a phototrophic bacterium to sediment microenvironments. *Proc Natl Acad Sci USA* 105: 18543-18548.

28. Ochman H, Gerber AS, Hartl DL (1988) Genetic applications of an inverse polymerase chain reaction. *Genetics* 120: 621-623.

29. Link AJ, Phillips D, Church GM (1997) Methods for generating precise deletions and insertions in the genome of wild-type *Escherichia coli*: application to open reading frame characterization. *J Bacteriol* 179: 6228-6237.

30. Friedrich CG, Bardischewsky F, Rother D, Quentmeier A, Fischer J (2005) Prokaryotic sulfur oxidation. *Curr Opin Microbiol* 8: 253-261.

31. 26. Rolls JP, Lindstrom ES (1967) Effect of thiosulfate on the photosynthetic growth of *Rhodopseudomonas palustris. J Bacteriol* 94: 860-866.

32. Varga AR, Staehelin LA (1983) Spatial differentiation in photosynthetic and non-photosynthetic membranes of *Rhodopseudomonas palustris. J Bacteriol* 154: 1414-1430.

33. Hungate, R.e. "Chapter IV A Roll Tube Method for Cultivation of Strict Anaerobes." *Methods in Microbiology* (1969): 117-32.

34. Yen KM (1991) Construction of cloning cartridges for development of expression vectors in gram-negative bacteria. *J Bacteriol* 173: 5328-5335.